

Broadly tunable LiInSe₂ optical parametric oscillator pumped by a Nd:YAG laser

Georgi Marchev,^{a)} Aleksey Tyazhev,^{a)} Vitaliy Vedenyapin,^{b)} Dmitri Kolker,^{c)}
Alexander Yelisseyev,^{b)} Sergei Lobanov,^{b)} Ludmila Isaenko,^{b)} Jean-Jacques Zondy,^{d)}
Valentin Petrov^{a)}

^{a)}Max-Born-Institute for Nonlinear Optics and Ultrafast Spectroscopy, 2A Max-Born-Str.,
D-12489 Berlin, Germany;

^{b)}Institute of Geology and Mineralogy, SB RAS, 43 Russkaya Str., 630058 Novosibirsk, Russia;

^{c)}Novosibirsk State Technical University, 20 K. Marx Pr., Novosibirsk, 630072, Russia and
Institute of Laser Physics (SB-RAS), 13/3 Lavren'teva Pr., Novosibirsk, 630090, Russia;

^{d)}Institut National de Métrologie, Conservatoire National des Arts et Métiers, 61 rue du Landy,
F-93210 La Plaine St Denis, France

ABSTRACT

LiInSe₂ is one of the few (in the meanwhile 6) non-oxide nonlinear crystals whose band-gap (2.86 eV) and transparency enabled in the past nanosecond optical parametric oscillation in the mid-IR without two-photon absorption for a pump wavelength of 1064 nm. However, the first such demonstration was limited to the 3.34-3.82 μm spectral range with a maximum idler energy of 92 μJ at 3.457 μm for a repetition rate of 10 Hz. Now we achieved broadly tunable operation, from 4.65 to 7.5 μm , with a single crystal, reaching maximum idler pulse energy of 282 μJ at 6.514 μm , at a repetition rate of 100 Hz (\sim 28 mW of average power).

Key words: optical parametric oscillators; nonlinear crystals; tunable mid-infrared radiation

1. INTRODUCTION

Although room temperature lasing has been reported up to \sim 5 μm , practical solid-state-lasers have an upper limit of \sim 3 μm , with the most prominent representatives being the fixed wavelength Er³⁺-lasers and the tunable Cr²⁺-lasers.¹ The main difficulty with such lasers consists not only in finding suitable laser transitions with long living upper state but also in the exotic pump lasers required. However, the spectral range above 3 μm in the mid-IR can be continuously covered by nonlinear frequency down-conversion using powerful laser sources in the near-IR. Oxide-based crystals, for example phosphates and arsenates belonging to the KTiOPO₄ (KTP) family of isomorphs, or iodates, niobates and tantalates like LiIO₃, LiNbO₃, KNbO₃, LiTaO₃, as well as all their periodically poled counterparts, can be pumped by widely-spread high-power diode-pumped laser systems, such as Nd:YAG, and perform well up to 4 μm , but their performance at longer wavelengths is dramatically affected by the onset of multi-phonon mid-IR absorption. Since nonlinear frequency conversion is intensity dependent process, high efficiency can be expected only using pulsed laser sources (femtosecond to nanosecond). At practical pump intensities, most of the chalcogenide mid-IR nonlinear crystals will suffer then two-photon absorption (TPA) at the pump wavelength of 1064 nm because of their low band-gap. Although TPA is the major limitation, in many cases residual absorption at the pump wavelength or insufficient birefringence for phase-matching represent additional constraints. Thus, from the I-III-VI₂ chalcopyrite crystals, only AgGaS₂ but not AgGaSe₂, can be phase-matched and pumped without TPA at 1064 nm, however, sulfides exhibit in general substantially lower second order nonlinearity than selenides. II-IV-V₂ chalcopyrites offer superior properties in comparison to the I-III-VI₂ chalcopyrite crystals in terms of nonlinearity, low scattering losses, hardness, and thermo-optical and thermo-mechanical

parameters, but even the most developed compound, ZnGeP₂, requires pump wavelengths near 2 μm (less common sources like Tm- or Ho-lasers) in order to avoid two-photon and residual absorption as well as to enable phase-matching. The TPA problem precludes also the pumping of the newly developed orientation-patterned GaAs at wavelengths near 1 μm. In fact, there are only few candidates for such down-conversion devices pumped near 1064 nm, the properties of which were compared in Ref. 2 taking into account the TPA, residual absorption, birefringence, effective nonlinearity, thermal conductivity, and limitations related to the growth, availability and some opto-mechanical properties.

Although femtosecond and picosecond pulses are associated with much higher peak intensities, it is difficult to achieve simultaneously high output energies and conversion efficiency because of limitations related to the spectral acceptance or higher order dispersion and nonlinear effects. Thus nanosecond optical parametric oscillators (OPOs) seem to possess the best potential for achieving high average power and single pulse energy. Such OPOs, pumped in the 1 μm range, have been demonstrated, however, only with 6 of the 14 compounds analyzed in Ref. 2: Ag₃AsS₃,³⁻⁵ AgGaS₂,⁶⁻⁹ HgGa₂S₄,¹⁰⁻¹¹ the solid solution Cd_xHg_{1-x}Ga₂S₄,¹²⁻¹³ LiInSe₂,¹⁴ and very recently CdSiP₂.¹⁵ The relevant properties of these crystals are summarized in Table 1, where a specific pump (1064 nm) and idler (6.45 μm) wavelengths are selected for comparison.

Table 1. Compilation of important properties of nonlinear crystals for which OPO operation with ~1 μm pump has already been demonstrated. The citations in column 2 refer to the Sellmeier equations used. The effective nonlinear coefficients d_{eff} (column 3) are calculated at the corresponding phase-matching angle θ or φ (column 2), the nonlinear tensor components, d_{ij} , used for this calculation were derived from the literature (column 6) applying Miller's rule (column 7). The wavelength λ_F (fundamental) at which the nonlinear coefficients have been estimated by SHG is also included in column 6. Citations in the first column refer to the whole row.

Crystal Point group [Reference]	Plane	$\theta / \varphi [^\circ]$ (Interaction)	d_{eff} [pm/V]	Thermal conductivity [W/mK]	Band- gap E_g [eV]	Miller's δ [pm/V] or d_{ij} [pm/V] @ λ_F for SHG	+ Miller's correction [pm/V]
AgGaS ₂ $\bar{4}2m$		40.50 (oo-e) 45.53 (eo-e) [16]	8.86 13.65	1.4 //c 1.5 \perp c [17]	2.70 [18]	$\delta_{36}=0.12$ [19]	$d_{36}=13.65$
HgGa ₂ S ₄ $\bar{4}$		45.87 (oo-e) 51.21 (eo-e) [10]	15.57 21.18	2.49-2.85 //c 2.36-2.31 \perp c [20]	2.79 [20]	$d_{36}=27.2$ @ 1064 nm [20]	$d_{36}=24.56$
Cd _x Hg _{1-x} Ga ₂ S ₄ ($\theta=90^\circ$, x=0.55) $\bar{4}$		90.00 (oo-e) [20]	24.94	1.8-1.92 //c 1.62-1.81 \perp c (x=0.27-0.3) [20]	3.22 (x=0.55) [20]	$d_{36}=27.2$ @ 1064 nm [20]	$d_{36}=24.94$
LiInSe ₂ $mm2$ [21]	xz xy	36.97 (oo-e) 41.62 (eo-e)	7.26 10.57	4.7-4.5 //x 4.7-4.8 //y 5.5-5.8 //z	2.86	$d_{31}=11.78$ $d_{24}=8.17$ @ 2300 nm	$d_{31}=12.08$ $d_{24}=8.65$
CdSiP ₂ $\bar{4}2m$		80.46 (oo-e) [22]	90.99	13.6 [2]	2.2-2.45 [23]	$d_{36}=84.5$ @ 4.56 μm [2]	$d_{36}=92.27$
Ag ₃ AsS ₃ $3m$ [24]		22.04 (oo-e) 24.01 (eo-e) 65.63 (oc-e)	22.89 16.44 3.35	0.113 //c, 0.092 \perp c	2.2	$d_{31}=10.4$ $d_{22}=16.6$ @ 10.6 μm	$d_{31}=12.34$ $d_{22}=19.70$

AgGaS₂ (AGS) is the only commercially available crystal from Table 1. Besides its modest nonlinearity, it exhibits low thermal conductivity and strongly anisotropic thermal expansion. HgGa₂S₄ shows improved nonlinearity but the growth of this crystal in large sizes with sufficient homogeneity is still problematic and several phases exist. Cd_xHg_{1-x}Ga₂S₄, with x=0.55 adjusted to have non-critical phase-matching for the selected process, is a solid solution in the system HgGa₂S₄ – CdGa₂S₄ and can be grown in larger sizes but its composition cannot be maintained constant. Li-compounds exhibit the largest band-gaps of all mid-IR crystals but their nonlinear coefficients are relatively low. Unlike the AGS chalcopyrite, they crystallize in the β -NaFeO₂ wurtzite-type structure (orthorhombic $mm2$ symmetry). The interest in LiInSe₂ (LISE), the Li compound with highest nonlinearity, is motivated by its superior thermo-mechanical properties:²¹ quasi-isotropic expansion, thermal conductivity ~5 W/mK (~3 times higher than in AGS), and smaller thermo-optic coefficients as well as higher damage threshold than AGS, which are important for average power scaling. Ag₃AsS₃

(proustite) is an archive crystal, included in Table 1 only for completeness. Being one of the first mid-IR crystals studied, its development has been cancelled in favor of the chalcopyrites such as AGS, because of the poor thermo-mechanical properties and low laser damage threshold. CdSiP₂ is a II-IV-V₂ chalcopyrite with negative birefringence whose growth technology was developed only very recently. It possesses unique properties for down conversion to the mid-IR at pump wavelengths near 1 μm and outperforms all other crystals in all aspects, not only those used for comparison in the table, but also in terms of hardness, damage threshold or anisotropy of the thermal expansion, as well as the possibility of non-critical phase-matching with maximized effective nonlinearity without being a solid solution. However, a practical upper limit of 6.5 μm for the idler wavelength can be assumed due to the onset of intrinsic multi-phonon absorption: This defines a potentially interesting spectral range of only 4 to 6.5 μm.

Table 2 summarizes the OPO results demonstrated so far with the 6 crystals from Table 1. Q-switched Nd:YAG lasers (Nd:CaWO₄ in Ref. 4,5) have been used for pumping. Simple two-mirror cavities were employed in all cases.

Table 2. Development of 1-μm pumped OPOs based on non-oxide materials. *L*: crystal length, SF: single-frequency, *T_p*: pump pulse duration (FWHM), SP: single pump pass, DP: double pump pass, N-C: non-collinear, Q-D: quasi-degeneracy, SR: singly resonant, DR: doubly resonant, NC: non-critical, NM: not measurable, λ_i : idler wavelength (tunability), *E_i*: maximum idler energy, *I_p*: maximum applied or damage level pump intensity. Cd_xHg_{1-x}Ga₂S₄ and CdSiP₂ operated under NC conditions with tuning by variable composition ($x=0.21-0.25$ in Ref. 13) in the case of Cd_xHg_{1-x}Ga₂S₄ and at fixed wavelength for CdSiP₂.

Crystal, Type	<i>L</i> [mm]	λ_p [nm], Mode	Rep. rate [Hz]	<i>T_p</i> [ns]	SP/DP	λ_i [μm]	<i>E_i</i> [μJ] @ λ_i	Peak <i>I_p</i> [MW/cm ²], Limits, comments	Year	[Ref.]
Ag ₃ AsS ₃ I (e-oo)	3.8	1064 TEM ₀₀	2000	200	SP	~2.128, Q-D, DR	NM	0.45, surface and/or coating damage	1970	[3]
Ag ₃ AsS ₃ I (e-oo)	10	1065 TEM ₀₀ , SF	2	26	SP	2.13-2.56 Q-D, DR	12.5 @ 2.13 μm	8.5, safe 19, surface damage	1972	[4]
Ag ₃ AsS ₃ I (e-oo)	10	1065 TEM ₀₀	2	25	SP, N-C	2.13-8.5, SR	2.5 @ 4.5 μm	see above	1973	[5]
AgGaS ₂ I (e-oo)	20	1064 TEM ₀₀	10	20	SP	2.128-4, SR	250 @ 2.128 μm	10, surface damage	1984	[6]
AgGaS ₂ I (e-oo)	20	1064	10	10.9	DP	2.77-4.2, SR	120 @ 3.5 μm	<30, surface damage after 50 shots	1997	[7]
AgGaS ₂ II (e-oe)	20	1064, TEM ₀₀	10	20- 30	DP	3.9-11.3, SR	372 @ 6 μm	10, surface damage	1999	[8]
AgGaS ₂ I (e-oo)	20	1064, TEM ₀₀	1	15	DP	2.6-5.3, SR	620 @ 4 μm	34, mirror damage	2006	[9]
HgGa ₂ S ₄ II (e-oe)	8	1064	10			~3.7-4.5, SR		40, surface damage	1998	[10]
HgGa ₂ S ₄ I (e-oo)	6	1064, TEM ₀₀	10	30	SP	2.3-4.4, SR	360 @ 2.37 μm	40, surface damage, single shot (extracavity) ²⁵	2003	[11]
Cd _x Hg _{1-x} Ga ₂ S ₄ I (e-oo)	10.9- 11.6 $x=0.22$ -0.56	1064, TEM ₀₀	10	30	SP	3.16-8.9, SR, NC for $x=0.56$	270 @ 5.76 μm 110 @ 8.9 μm	damage threshold: 6 fold that of AGS $x=0.35$ (extracavity) <i>T_p</i> =9 ns, single shot	2004	[12]
Cd _x Hg _{1-x} Ga ₂ S ₄ I (e-oo)	11 $x=0.21$ -0.25	1064, TEM ₀₀	10	22	SP	2.85-3.27, SR, NC	400 @ 3.03 μm		2005	[13]
LiInSe ₂ II (e-oe)	17	1064	10	10	DP	3.34-3.82, SR	92 @ 3.457 μm	40, safe (extracavity) 54, coating damage ²⁶	2005	[14]
LiInSe ₂ II (e-oe)	17.6	1064	100	14	DP	4.65-7.5, SR	282 @ 6.5 μm	>21, surface damage limit (intracavity) 45, coating damage (extracavity)	2009	This work
CdSiP ₂ I (e-oo)	8	1064	10	14	DP	6.2, SR, NC	470 @ 6.2 μm	25, AR coating damage (intracavity)	2009	[15]

In this work we report broadband operation of a 1064 nm pumped LiSe OPO, tunable from 4.65 to 7.5 μm using a single crystal sample. Pumping at a repetition rate of 100 Hz and the absence of thermal effects enabled us to increase the average power by more than an order of magnitude at wavelengths much longer than in the initial demonstration.¹⁴

2. EXPERIMENTAL SETUP AND CRYSTAL SAMPLE

The OPO cavity used is shown in Figs. 1 and 2. It consisted of two plane mirrors with a separation between 18.5 and 20.5 mm. The rear total reflector, TR, was an Ag-mirror (Balzers) with a reflection of $>98.5\%$ at the pump, signal and idler wavelengths. In the tuning range studied in the present work, the output coupler, OC, had a transmission of 18-22% at the signal and ~ 73 -84% at the idler wavelength, hence, the OPO can be considered as singly resonant with double pass pumping. However, the signal was not totally reflected by the output coupler to avoid extreme intracavity fluence that could damage the crystal. The LiSe crystal was pumped through the output mirror which had a transmission of 82% at 1064 nm. The beams were separated by the pump bending mirror, BM, which had high reflection for the pump ($R=98\%$ for p-polarization) and transmitted $\sim 67\%$ (p-polarization) at the idler wavelengths, respectively. Both the plane-parallel output coupler, OC, and the bending mirror, BM, were on ZnSe substrates with uncoated rear surfaces.

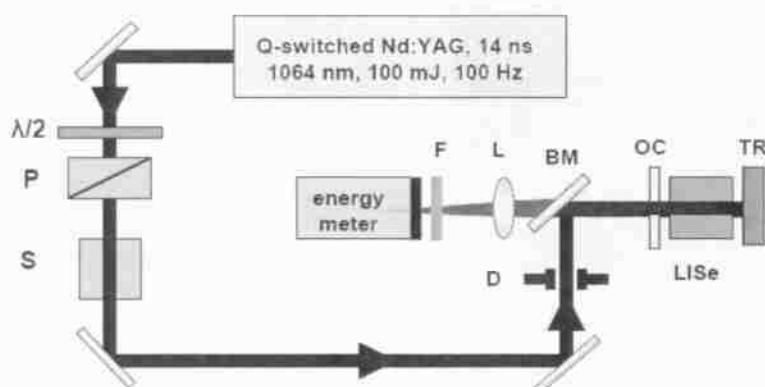


Fig. 1 Experimental setup of the LiSe OPO. $\lambda/2$: half-wave plate, P: polarizer, S: mechanical shutter, F: 2.5 μm cut-on filter, L: 10 cm MgF_2 lens, D: diaphragm, BM: bending mirror, OC: output coupler, TR: total reflector.

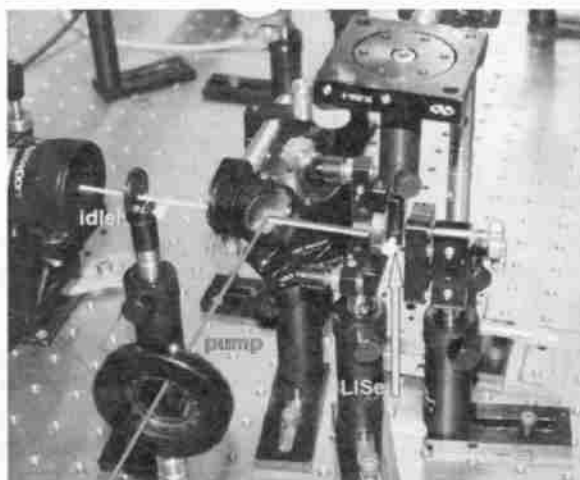


Fig. 2 Photograph of the compact OPO setup.

The pump source was a diode-pumped, electro-optically Q-switched Nd:YAG laser (Innolas GmbH, Germany) optimized for a repetition rate of 100 Hz. According to the specifications, its linewidth amounts to 1 cm^{-1} , M^2 is <1.5 and the divergence is $<0.5 \text{ mrad}$. The laser generated 100 mJ, 14 ns (FWHM) pulses with an average power of 10 W. The measured energy stability was $\pm 1\%$.

A mechanical shutter (S) with an aperture of 8 mm, operating up to 50 Hz (nmLaser), was employed to reduce the repetition rate and thus the average pump power. A combination of a half-wave plate, $\lambda/2$, and a polarizer, P, served to adjust the pump energy. The pump laser was protected by a Faraday isolator and the separation to the OPO was large enough to avoid feedback during the Q-switching process. The pump beam was not focused and had a Gaussian waist of $w=1.9 \text{ mm}$ in the position of the OPO. The output of the OPO, behind the bending mirror, BM, was detected by a calibrated pyroelectric energy meter positioned in front of the focus of a 10-cm MgF_2 lens, L. Only the idler energy was measured, the residual pump radiation and the signal were blocked by a $2.5 \mu\text{m}$ cut-on filter, F.

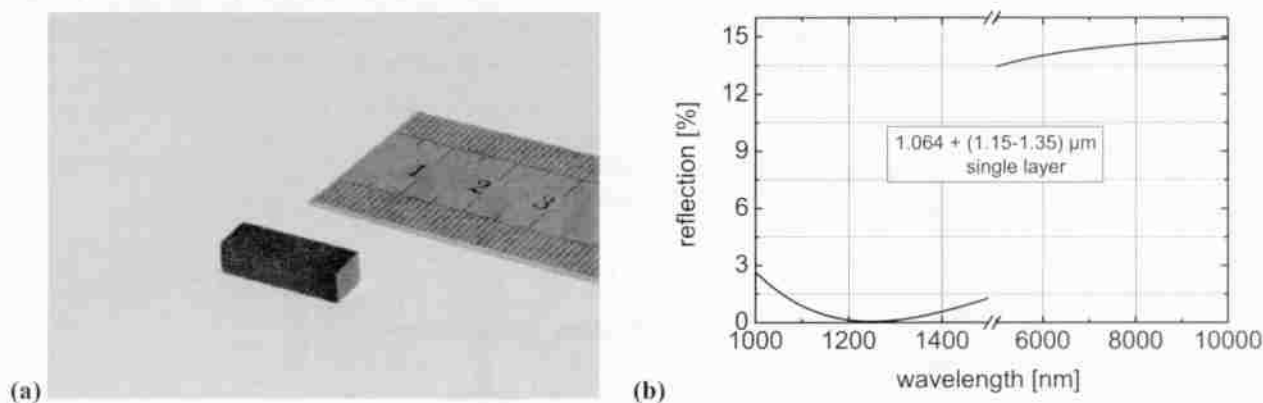


Fig. 3. AR coated sample of LiInSe_2 used in the present work (a) and the single-layer AR-coating design (b).

The sample used in the present study, see Fig. 3a, was grown from an oriented seed by the vertical two-zone furnace Bridgman technique. It was cut for propagation in the x - y plane, type-II e-oe phase-matching, which is characterized by maximum effective nonlinearity, d_{eff} .²¹ The azimuthal angle cut was at $\varphi=41.6^\circ$ for idler wavelength $\sim 6.5 \mu\text{m}$ at normal incidence. The aperture was 5 mm (along z -axis) \times 6.5 mm and the length was 17.6 mm. The sample was AR-coated with a single layer of YF_3 for high transmission at 1064 nm and in the 1.15-1.35 μm signal range (Fig. 3b). The residual reflectivity of the two surfaces was, however, different, with average values of 2.8% at 1064 nm and 1.8% at 1600 nm. From the measured transmission of 71% at 1064 nm and 85% at 1600 nm, we estimated effective absorption (including scatter) of 16%/cm at 1064 nm and 7%/cm at 1600 nm.

3. RESULTS AND DISCUSSION

We studied the input/output characteristics of the OPO, including the oscillation threshold, at normal incidence and minimum possible cavity length (18.5 mm). The tuning curve required tilting of the crystal and the corresponding cavity length was slightly increased (20.5 mm).

The threshold amounted to 6.8 mJ, energy incident on the crystal. This value corresponds to an average fluence of 0.06 J/cm^2 or pump intensity of 4.3 MW/cm^2 . The peak on-axis values for the fluence and the intensity are two times higher. The threshold can be calculated by using Brosnan & Byer's formula²⁷ for a singly resonant OPO with recycled pump. We used the exact experimental parameters, correcting for the pump beam absorption after the first pass and assuming equal (averaged for signal and idler) absorption of 5%/cm for the resonated wave. From the nonlinear coefficients of LiSe , rescaled using Miller's rule,² we calculated an effective nonlinearity of $d_{\text{eff}}=10.6 \text{ pm/V}$ ($\varphi=41.6^\circ$), see Table 1. The result for the threshold pump fluence was 0.23 J/cm^2 . This value correlates better with the experimental

peak (on-axial) fluence which can be explained by the fact that oscillation starts in the central part of the pump beam. Deviations may have several reasons: the losses at the exact signal and idler wavelengths were unknown and we interpolated them to 6%/cm at the signal and assumed 4%/cm at the idler wavelength in accordance with Ref. 14, eventually these losses could be higher; besides for the pump, the residual reflections at the crystal faces were neglected; and finally the partial resonance of the idler is not taken into account by the theory. Having in mind all such assumptions, the correspondence between theory and experiment can be considered as satisfactory.

At a pump level of about two times the pump threshold we investigated the dependence of the output power on the repetition rate in the range 10-100 Hz. Fluctuations were within the experimental error and we conclude that there is no such dependence. This result was rather unexpected since the present sample had in fact larger residual absorption than the one used in the initial work¹⁴ at shorter idler wavelengths. This fact can be explained by the weaker thermal lensing in the case of larger beam sizes. The further measurements were performed at 100 Hz with the shutter removed (Fig. 1).

The input/output characteristics are shown in Fig. 4. Maximum energy of 282 μJ at 6.514 μm was measured. This value corresponds to an external quantum conversion efficiency of 10.3%. The above wavelength deviates from the calculated one being slightly longer. However, the deviation at the signal wavelength, from the measurement of which the idler wavelength was calculated, was only about 3 nm. The maximum average power at 100 Hz amounts to 28 mW. This is an improvement of more than an order of magnitude in comparison to our initial work, where ~ 2.5 mW at 3.457 μm were achieved at lower repetition rates.¹⁴ Since OPO operation with any chalcogenide crystal is confined to a narrow pump power range between the oscillation threshold and the damage threshold, this fact emphasizes the importance of the good spatial profile and the pulse-to-pulse stability of the diode-pumped pump source.

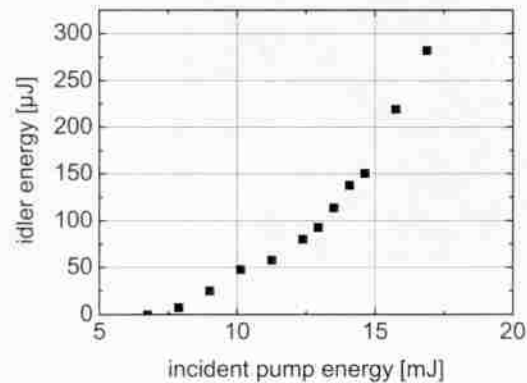


Fig. 4. Output idler energy versus pump energy at 1064 nm, incident on the crystal. The curve is recorded at normal incidence with a cavity length of 18.5 mm. The idler wavelength is 6.514 μm .

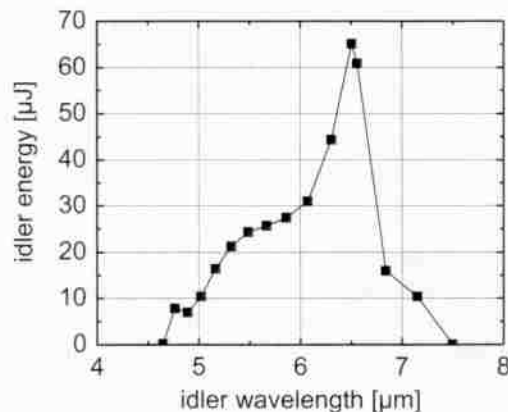


Fig. 5. Tuning OPO curve recorded for a cavity length of 20.5 mm at fixed pump energy.

The OPO linewidth was measured at the signal wavelength of 1272 nm using a 1-mm-thick Ag-coated CaF₂ Fabry-Perot etalon. It was ~58 GHz (~1.9 cm⁻¹). This is 2 times less than the spectral acceptance for the three-wave nonlinear process assuming narrow-band pump. The pulse-to-pulse stability for the idler pulses measured at maximum output level was +/- 5%. The pulse duration at the same signal wavelength, measured with a fast (0.7 ns) InGaAs photodiode, was 7 ns.

The tuning curve (Fig. 5) was recorded by tilting the crystal in the critical plane (rotation about the z-axis). The pump energy was 11.8 mJ. As can be seen, we achieved substantial extension of the tunability range of the LISe OPO pumped at 1064 nm. The sharp peak at normal incidence can be attributed to the residual crystal reflections.

The lowest pump level at which surface damage in the form of whitened spots on the coating (or beneath it), were observed, was a peak on-axial pump intensity of 16 MW/cm². This corresponds to operation roughly two times above the threshold and strong signal field is already present in the cavity. By translating the sample in transversal direction, we observed several times the same kind of damage to the same surface, the one with higher residual reflectivity of the AR-coating, independent of the orientation of the sample with respect to the pump beam (entrance or exit surface). No damage occurred to the other surface of the sample.

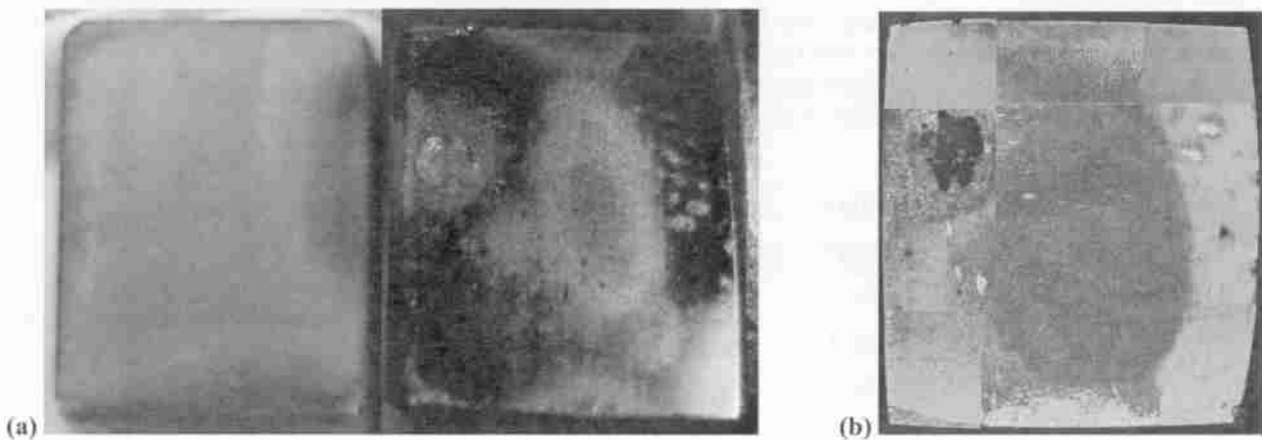


Fig. 6. Lower-reflecting (left) and higher-reflecting (right) surface of the damaged LISe OPO element (a) and 12 microscope images of the severely damaged higher-reflecting surface combined into a single picture.

The same sample was studied for damage also extracavity, using the same pump source and fresh positions. The tests were performed for 60 s (6000 shots). Again the same surface had low damage threshold although it was always an exit surface. The damage threshold for the occurrence of similar whitened spots was 23 MW/cm². Full damage to this surface (coating destroyed and crater appeared, see Fig. 6a) occurred at 45 MW/cm². At this same intensity level, the first whitened spot on the other surface (the one with lower residual reflectivity) was observed. Hence, this value is included in Table 2 as a realistically achievable damage resistivity level of this type of coating.

No reliable information could be obtained on gray track formation which seems not to be the limiting factor in the temporal regime studied. However, many point defects could be seen with a microscope, inside the bulk and on the surface (Fig. 6b).

In principle, the AR-coating applied seems to be sufficiently resistant for OPO operation. But the quality of the coating is not reproducible as evidenced by the OPO experiment, in which always one of the surfaces (the one with higher residual reflectivity) got damaged at lower pump levels. This could be attributed to the fact that after AR-coating one of the surfaces, the other one was not polished. In the future we plan to polish the two crystal faces independently prior to their coating.

The damage of the OPO sample in the form of whiter surface spot occurred at lower pump energy (14.4 mJ) when inside the cavity in comparison to the use extracavity (20 mJ) which emphasizes the contribution of the resonated signal wave.

Nevertheless, the presence of such spots did not affect the OPO performance until the damage developed further as can be seen from Fig. 4. Once the problem with the reproducibility of the AR-coating is solved one can expect substantial improvement of the OPO performance.

4. CONCLUSION

In summary, we demonstrated for the first time to our knowledge nanosecond OPO operation with LiSe crystal in the mid-IR wavelength range above 4 μm extending up to 7.5 μm for the idler wave. The maximum idler pulse energy of 282 μJ at $\sim 6.5 \mu\text{m}$ corresponds to an average power of $\sim 28 \text{ mW}$ at a repetition rate of 100 Hz. This compares well with the 372 μJ at 6 μm reported with an AGS OPO.⁸ Further scaling is possible provided better polishing and AR-coating processes are developed. One of main challenges, however, remains the reduction of the residual losses in the clear transparency range of LiSe because only after solving this problem the better thermo-mechanical characteristics of this material will allow to outperform the more conventional chalcopyrite AGS.

ACKNOWLEDGMENTS

The research leading to these results has received funding from the European Community's Seventh Framework Programme FP7/2007-2011 under grant agreement n° 224042. We acknowledge also support from DLR (International Bureau of BMBF) under project RUS 08/013 and from DAAD, Michail-Lomonosov-Programme (D. K.).

REFERENCES

- ¹ A. A. Kaminskii, "Laser crystals and ceramics: recent advances," *Laser & Photon. Rev.* **1**, 93-177 (2007).
- ² V. Petrov, F. Noack, I. Tunchev, P. Schunemann, and K. Zawilski, "The nonlinear coefficient d_{36} of CdSiP_2 ," *Proc. SPIE* **7197**, 7197-21/1-8 (2009).
- ³ E. O. Amman and J. M. Yarborough, "Optical parametric oscillation in proustite," *Appl. Phys. Lett.* **17**, 233-235 (1970).
- ⁴ D. C. Hanna, B. Luther-Davies, H. N. Rutt, and R. C. Smith, "Reliable operation of a proustite parametric oscillator," *Appl. Phys. Lett.* **20**, 34-36 (1972).
- ⁵ D. C. Hanna, B. Luther-Davies, and R. C. Smith, "Singly resonant proustite parametric oscillator tuned from 1.22 to 8.5 μm ," *Appl. Phys. Lett.* **22**, 440-442 (1973).
- ⁶ Y. X. Fan, R. C. Eckardt, and R. L. Byer, "AgGaS₂ infrared parametric oscillator," *Appl. Phys. Lett.* **45**, 313-315 (1984).
- ⁷ P. B. Phua, R. F. Wu, T. C. Chong, and B. X. Xu, "Nanosecond AgGaS₂ optical parametric oscillator with more than 4 micron output," *Jpn. J. Appl. Phys.* **36**, L1661-L1664 (1997).
- ⁸ K. L. Vodopyanov, J. P. Maffetone, I. Zwieback, and W. Rudermann, "AgGaS₂ optical parametric oscillator continuously tunable from 3.9 to 11.3 μm ," *Appl. Phys. Lett.* **75**, 1204-1206 (1999).
- ⁹ T.-J. Wang, Z.-H. Kang, H.-Z. Zhang, Q.-Y. He, Y. Qu, Z.-S. Feng, Y. Jiang, J.-Y. Gao, Y. M. Andreev, and G. V. Lanskii, "Wide-tunable, high energy AgGaS₂ optical parametric oscillator," *Opt. Express* **14**, 13001-13006 (2006).
- ¹⁰ E. Takaoka and K. Kato, "Tunable IR generation in HgGa₂S₄," Conference on Lasers and Electro-Optics CLEO'98, San Francisco (CA), USA, May 3-8, 1998, paper CWF39, 1998 OSA Technical Digest Series Vol. 6, pp. 253-254.
- ¹¹ V. V. Badikov, A. K. Don, K. V. Mitin, A. M. Seregin, V. V. Sinaiskii, and N. I. Schebetova, "A HgGa₂S₄ optical parametric oscillator," *Quantum Electron.* **33**, 831-832 (2003) [transl. from *Kvantovaya Elektron.* **33**, 831-832 (2003)].

- ¹² V. Badikov, A. Fintisova, V. Panutin, S. Sheina, S. Scherbakov, G. Shevyrdyaeva, A. Don, K. Mitin, N. Schebetova, A. Seryogin, V. Sinaisky, N. Kuzmin, V. Laptev, A. Malinovsky, E. Ryabov, J. Mangin, G. Gadret, J.-C. Jules, G. Mennerat, C. Pasquer, and J.-C. de Miscault, "Hg_{1-x}Cd_xGa₂S₄ crystals as new materials for mid-infrared parametric oscillators pumped by Nd:YAG lasers," Conference on Lasers and Electro-Optics CLEO'04, San Francisco (CA), USA, May 16-21, 2004, paper CThT44, CLEO/IQEC Technical Digest CD-ROM.
- ¹³ V. V. Badikov, A. K. Don, K. V. Mitin, A. M. Seryogin, V. V. Sinaiskiy, and N. I. Schebetova, "Optical parametric oscillator on an Hg_{1-x}Cd_xGa₂S₄ crystal," *Quantum Electron.* **35**, 853-856 (2005) [transl. from *Kvantovaya Elektron.* **35**, 853-856 (2005)].
- ¹⁴ J.-J. Zondy, V. Vedenyapin, A. Yelisseyev, S. Lobanov, L. Isaenko, and V. Petrov, "LiInSe₂ nanosecond optical parametric oscillator," *Opt. Lett.* **30**, 2460-2462 (2005).
- ¹⁵ V. Petrov, P. G. Schunemann, K. T. Zawilski, and T. M. Pollak, "Non-critical singly resonant OPO operation near 6.2 μm based on a CdSiP₂ crystal pumped at 1064 nm," *Opt. Lett.* **34**, 2399-2401 (2009).
- ¹⁶ E. Takaoka and K. Kato, "Thermo-optic dispersion formula for AgGaS₂," *Appl. Opt.* **38**, 4577-4580, 1999.
- ¹⁷ J. D. Beasley, "Thermal conductivities of some novel nonlinear optical materials," *Appl. Opt.* **33**, 1000-1003, 1994.
- ¹⁸ A. Jayaraman, V. Narayanamurti, H. M. Kasper, M. A. Chin, and R. G. Maines, "Pressure dependence of the energy gap in some I-III-VI₂ compound semiconductors," *Phys. Rev. B* **14**, 3516-3519, 1976.
- ¹⁹ J.-J. Zondy, D. Touahri, and O. Acef, "Absolute value of the d₃₆ nonlinear coefficient of AgGaS₂: prospect for a low-threshold doubly resonant oscillator-based 3:1 frequency divider," *J. Opt. Soc. Am.* **14**, 2481-2497, 1997.
- ²⁰ V. Petrov, V. Badikov, and V. Panyutin, "Quaternary nonlinear optical crystals for the mid-infrared spectral range from 5 to 12 micron," In: *Mid-Infrared Coherent Sources and Applications*, ed. by M. Ebrahim-Zadeh and I. Sorokina, *NATO Science for Peace and Security Series - B: Physics and Biophysics*, Springer (2008), pp. 105-147.
- ²¹ J.-J. Zondy, V. Petrov, A. Yelisseyev, L. Isaenko, and S. Lobanov, "Orthorhombic crystals of lithium thioindate and selenoindate for nonlinear optics in the mid-IR," In: *Mid-Infrared Coherent Sources and Applications*, ed. by M. Ebrahim-Zadeh and I. Sorokina, *NATO Science for Peace and Security Series - B: Physics and Biophysics*, Springer (2008), pp. 67-104.
- ²² P. G. Schunemann, K. T. Zawilski, T. M. Pollak, V. Petrov, and D. E. Zelmon, "CdSiP₂: a new nonlinear optical crystal for 1 and 1.5-micron-pumped, mid-IR generation," *Advanced Solid-State Photonics*, Denver (CO), USA, Feb. 1 - 4, 2009, Conference Program and Technical Digest, Paper TuC6.
- ²³ A. Shileika, "Energy band structure and modulation spectra of A²B⁴C⁵ semiconductors," *Surf. Sci.* **37**, 730-747, 1973.
- ²⁴ D. N. Nikogosyan, *Nonlinear Optical Crystals: A Complete Survey*, Springer (2005).
- ²⁵ V. V. Badikov, N. V. Kuzmin, V. B. Laptev, A. L. Malinovsky, K. V. Mitin, G. S. Nazarov, E. A. Ryabov, A. M. Seryogin, and N. I. Schebetova, "A study of the optical and thermal properties of nonlinear mercury thiogallate crystals," *Quantum Electron.* **34**, 451-456 (2004) [transl. from *Kvantovaya Elektron.* **34**, 451-456 (2004)].
- ²⁶ J.-J. Zondy, A. Yelisseyev, S. Lobanov, L. Isaenko, V. Petrov, F. Noack, and F. Rotermund, "LiInSe₂ nanosecond optical parametric oscillator," Conference on Lasers and Electro-Optics CLEO'05, Baltimore (MD), USA, May 22-27, 2005, paper CThQ5, CLEO/QELS Technical Digest CD-ROM.
- ²⁷ S. J. Brosnan and R. L. Byer, "Optical parametric oscillator threshold and linewidth studies," *IEEE J. Quantum Electron.* **QE-15**, 415-431 (1979).